Langmuir

Article

pubs.acs.org/Langmuir

From Chain Collapse to New Structures: Spectroscopic Properties of Poly(3-thiophene acetic acid) upon Binding by Alkyl Trimethylammonium Bromide Surfactants

I. Echavarri Franco, P. Lorchat, J.-P. Lamps, M. Schmutz, A. Schröder, J.-M. Catala, J. Combet,[†] and F. Schosseler*

Institut Charles Sadron, CNRS-University of Strasbourg, 23 rue du Loess, BP 84047, 67034 Strasbourg Cedex 2, France

Supporting Information

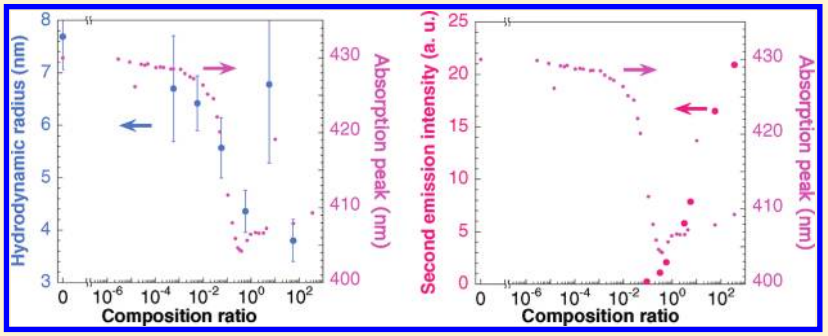

ABSTRACT: The binding of cationic surfactants with varying alkyl chain length to a regiorandom conjugated polyanion, poly(3-thiophene acetic acid) (PTAA), is studied in an aqueous buffer by using absorption and emission spectroscopies, photon correlation spectroscopy, isothermal titration calorimetry, and cryogenic transmission electron microscopy. We study the mixed solutions as a function of composition ratio R of surfactant molecules to monomer units molar concentrations, at low polymer concentration and in a very wide composition range ($10^{-6} < R < 10^{2}$) below the critical micellar concentration. Upon surfactant binding, the molecularly dispersed chains first collapse progressively and then form new structures as the mixed aggregates get enriched in surfactant. The collapse leads to a strong decrease of the conjugation length and to a blue shift of the absorption spectra by 30 to 50 nm. The new structures are responsible for a new intense emission band at about 600 nm, red-shifted by nearly 130 nm from the initial emission maximum of the polymer (~472 nm). As the surfactant tail becomes shorter, the blue shift of the absorption spectra and the intensity raise of the new emission are delayed to larger composition ratios while their variations become smoother functions of the surfactant concentration. These particular spectroscopic properties of PTAA seem related to its unique combination of a strongly hydrophobic backbone, a large ratio of contour length to persistence length, and an overall good aqueous solubility. Our results show that such features are well suited to design a colorimetric biosensor at small composition ratio, and a fluorescent biomarker at large composition ratio.

INTRODUCTION

Conjugated polyelectrolytes (CPEs) are a new class of polymer materials showing great promises for the design of both sensitive and selective biosensors in aqueous media.[1−5] This sensitivity is based on their spectroscopic properties depending strongly on their environment. Specific responses can be obtained by appropriate substitution of the conjugated polymer backbone resulting in fluorescence turn-off or turn-on upon binding with a specific substrate.[1]

Very promising selectivity was also demonstrated with nonspecifically substituted CPEs.[3,6−9] Many parameters can affect the spectroscopic properties of conjugated polymers. In particular the average conformation of the chains plays a well-known role on the overlap of 2p orbitals and the average conjugation length of the π electrons that are responsible for the spectroscopic properties of isolated conjugated polymers.[10−14] Intra- and interchain interactions as well as interactions with a substrate are also known to affect the spectroscopic properties of CPEs since Coulombic, hydrophobic, and van der Waals interactions as well as H-bonding can influence the delocalization of the π electrons along the backbone. The interplay of all of these factors is likely at the origin of the selective spectroscopic response of CPEs in the presence of a given substrate. However we still lack a comprehensive understanding of this interplay and there is a need for experimental studies with model systems to identify relevant parameters and foster theoretical work on these phenomena.[2−5]

One possible candidate for such a model system would be the mixture of oppositely charged surfactants/CPEs in aqueous

Received: December 9, 2011
Revised: February 13, 2012
Published: February 14, 2012

   dx.doi.org/10.1021/la204862u | Langmuir 2012, 28, 4815−4828

solutions. In the case of polyelectrolytes with a saturated backbone more than thirty years of extensive investigation about similar systems have brought a large body of experimental results as well as a rather wide consensus about their interpretation.[15−38] Therefore mixed oppositely charged surfactant/CPE solutions might constitute ideal systems where the interplay of Coulombic and hydrophobic interactions could be inferred from the existing literature on nonconjugated systems, thus facilitating the interpretation of spectroscopic behavior of CPEs in mixed solutions.

In fact the interest of surfactants as formulation additives in CPE-based sensors was pointed out at the very beginning of their development[39,40] and so-called surfactochromicity[41] was reported for CPEs based on poly(phenylene vinylene) (PPV),[39,40,42−44] poly(phenylene ethynylene) (PPE),[45−50] poly(fluorene phenylene) (PFP),[51−55] and poly(thiophene) (PT)[56−61] backbones.

For CPEs based on rigid PPE backbone, it is very difficult to obtain molecularly dispersed chains in aqueous solution and the addition of surfactants promotes the dispersion of the aggregates formed by the weakly soluble conjugated chains.[46−50] The increase in added surfactant concentration enhances the fluorescence while the emission spectra maximum shift to smaller wavelengths and exhibit vibronic features that are characteristic of isolated chains.[46−50] Absorption spectra shift similarly to smaller wavelengths.[47,49] Large values of molar ratio of surfactant to repeating units are often used to observe these effects.

Oligomers (degree of polymerization DP = 9) based on rigid PFP backbone exhibit fluorescence quenching for moderate surfactant concentration and fluorescence enhancement when the surfactant concentration is increased above the critical micellar concentration (cmc),[51,52,54] while the presence of surfactant has only small effects on the positions of the absorption (λ_{abs}) and emission (λ_{em}) maxima.[51,52,54] For longer polymer chains (DP = 35) the same trends for the fluorescence intensity are observed with a modest nonmonotonic variation in λ_{abs} and λ_{em}.[53] These effects are shifted to smaller surfactant concentration when the length of its hydrophobic tail is increased.[53]

In the case of more flexible PPV-based CPEs, small quantities of added surfactant yield a large enhancement of fluorescence intensity by a factor of about 20 accompanied by a blue shift and a structuration of the emission spectra.[39,40,42,44] Interestingly, these effects are reversed when the density of charged substituants is decreased by a factor 2.[43] Small angle neutron scattering experiments with a similar CPE at higher polymer and surfactant concentrations suggest that the addition of surfactant breaks the chains aggregates.[62]

Finally only a few studies have addressed the spectroscopic properties of PT-based CPEs dilute solutions in the presence of added surfactant.[56,57] The surfactants are added in large excess with respect to the polymer repeat units and the photoluminescence behavior depends on the length of the alkyl tails. For premicellar surfactant concentrations, quenching occurs with short tail surfactants while the photoluminescence is enhanced with long tail surfactants. This is interpreted as the formation of polymer−surfactant aggregates with morphologies depending on the tail length, longer tails favoring the separation of chains and decreasing $\pi-\pi$ interchain interactions. At higher surfactant concentrations, close to their cmc, chain aggregation is inhibited and photoluminescence increases for all surfactant tails by a factor close to 3 with respect to the pure polymer value.[57] The modulation of photoluminescence intensity is associated with a moderate (<10 nm) nonmonotonic variation of its position λ_{em}, first increasing then decreasing with surfactant concentration. The absorption spectra tend to red-shift monotonically as the surfactant concentration increases.[57]

Thus, to summarize general trends from earlier studies, for small values ($R \approx 0.1$) of the composition ratio R defined as the ratio of molar concentrations of surfactant to polymer repeat units, enhanced[39,40] or quenched[51−53] fluorescence can be observed depending on the flexibility of the backbone. In this regime, the emission spectra are more sensitive to added surfactant when the ratio of persistence length to contour length of the chains is decreased.[39,40,51−53] As the composition ratio becomes closer to 1, aggregation effects dominate and quenching can be observed for short surfactants that favor shorter interchain distances within the mixed aggregates. For surfactant concentration above the cmc, chain aggregation is inhibited and fluorescence intensity tends to increase. The rigidity of the chains,[39,40,46−52,54] their charge density,[53] and the surfactant tail length[53,57] are critical parameters that can strongly modify the surfactochromic behavior.

Despite these many interesting earlier results, no previous work used mixed CPE−surfactants systems as model systems to investigate specifically the interplay between Coulombic and hydrophobic interactions. In many cases, surfactant concentrations close to or above the cmc were used and the spectroscopic properties were dominated by the modulation of interchain interactions through aggregation/redissolution phenomena. Moreover only one study[44] varied the composition ratio in a large range $0.05 < R < 1000$. Therefore, the problem of understanding how dilute CPE solutions can detect minute amounts of a binding ligand was not specifically addressed.

Here we report on the spectroscopic behavior of a PT-based weak polyacid upon binding by cationic surfactants with varying alkyl chain length in buffered solution (pH 9.7). The composition ratio is varied in a large range ($10^{-6} < R < 10^{2}$) and the polymer concentration is low enough to keep the surfactant concentration below the cmc. The choice of a PT backbone is motivated by the good selectivity displayed by this type of CPE.[3,6−9] Moreover previous studies[63] on our specific sample, a nonregioregular poly(3-thiophene acetic acid) with DP ≈ 125, have shown that it is less prone to aggregation than other CPEs and that its conformational transition upon pH variation can be followed by absorption spectroscopy.[64] Therefore we anticipate a good solubility prior to surfactant addition and the possibility to follow the effect of surfactant binding on the spectroscopic properties of individual chains.

EXPERIMENTAL SECTION

1. Samples. The polymer sample is a regiorandom poly(3-thiophene acetic acid) (PTAA) with a degree of polymerization DP ≈ 125 and a polydispersity index around 2.2. Its synthesis and characterization have been detailed previously.[63]

Alkyl trimethylammonium bromide surfactants were purchased from Aldrich. In this study we used surfactants containing n = 6 (HTAB), 8 (OTAB), 10 (DeTAB), 12 (DoTAB), 14 (TTAB), and 16 (CTAB) carbons in the alkyl chain. We used also tetramethylammonium bromide as an extrapolation of n to 1 for this series. Except for DoTAB, that was recrystallized 3 times in a 1:24 mixture of ethanol and acetone, they were used as received.

Sample solutions were prepared in a sodium bicarbonate buffer (pH 9.7, ionic strength 36 mM). In these conditions the polymer chains can be considered as fully neutralized and have their highest effective

dx.doi.org/10.1021/la204862u | Langmuir 2012, 28, 4815−4828

ionization degree. The buffer aqueous solution was prepared with fresh milli-Q water and kept under Ar atmosphere.

A fixed polymer concentration C_p = 0.176 mM was used for most experiments with added surfactant. This choice is a best compromise with many advantages: with this low polymer concentration, interchain aggregation effects are minimized, surfactants are always below their cmc, whatever the R values, and the use of absorption and emission spectroscopy as well as photon correlation spectroscopy is possible, with some care however. Some complementary results have been obtained at higher polymer concentrations with samples prepared along the same lines.

To prepare the solutions of well-defined polyelectrolyte−surfactant composition, the aqueous stock solution of the polymer (C_p = 8.8 mM, pH ∼5, salt free solution) was diluted in the buffer to obtain a sample with a concentration close to the final one. A small amount of a stock buffered solution of the surfactant was then added to obtain the desired composition ratio R of surfactant to monomer molar concentrations ($10^{-3} \leq R \leq 360$) and the correct final polymer concentration. The solution was stirred at 250 rpm for one hour under Ar flux and then kept under inert atmosphere until the measurements were performed.

For titration experiments, an initial volume of 50 mL of polyelectrolyte in buffer solution was prepared. The surfactant from appropriate buffered stock solutions was then added stepwise. After waiting 3 min while bubbling Ar and stirring, the UV−visible absorption spectrum was measured in situ with a separate probe (Hellma). The pH was checked to be stable within 0.1 unit during the whole titration procedure. The change in the polymer concentration due to the addition of surfactant was about 6% for the range $10^{-6} < R < 100$.

The use of a buffered solution with an ionic strength equal to 36 mM ensures that the total ionic strength does not change upon surfactant addition by more than a few percent for most composition ratios. All experiments were performed at a temperature $T \approx 25$ °C, except for those with CTAB where T was set to 30 °C to prevent artifacts due to the low Krafft temperature of this surfactant. We checked that titration experiments with DoTAB performed at T = 25 and 30 °C were not sensitive to this difference in temperature.

2. UV−Visible Spectroscopy. UV−visible absorption curves were measured with a Cary 500 spectrometer either in standard quartz cells with an optical path of 10 mm (Hellma OS) or with an in situ probe (Hellma) having an optical path of 5 or 10 mm for the titration experiments. In the latter case, the dilution of the polymer after surfactant addition was taken into account for the determination of the maximum absorbance. Measurement were performed from 300 to 800 nm. Absorbance from pure buffer solution was systematically subtracted from sample solution absorption curves. The wavelength at maximum absorbance λ_{abs} was determined by a parabolic fit of the absorption values ranging above 90% of the maximum value. The absolute error on λ_{abs} values determined in this way was about ±0.2 nm (see the Supporting Information).

3. Emission Spectroscopy. Experiments were performed with a FluoroMax4 (Horiba-Jobin-Yvon) using standard cells with an optical path of 10 mm (Hellma). The entrance slit and the output slit were both set to allow a 5 nm resolution. Emission from pure buffer solution was subtracted from sample emission measurements.

Emission spectra of our polymer highly diluted in the buffer exhibit one broad peak that depends slightly on the excitation wavelength λ_{exc} (see the Supporting Information). Similar behavior has been reported and discussed for poly(phenylene vinylene) derivatives.[65−70] It is usually attributed to the presence of different chromophores, i.e., chain segments with different conjugation length, along the polymer backbone. This heterogeneity is linked to the intrinsic conformational disorder of the polymer chain. In this picture, shorter wavelength excitation can trigger emission from a larger continuum of chromophores. If the energy transfer from higher energy chromophores to lower energy chromophores is not very efficient, new features can even appear in the emission spectra for short excitation wavelengths. In the following the excitation wavelength was set to λ_{exc} = 373 nm, i.e., a value where the emission curves have a high intensity level and a shape independent of the excitation wavelength.

For polymer concentrations larger than C_p = 8.8 μM, inner filter effects[71−73] are already present and the emission intensity does not increase linearly with C_p. However we found they can be corrected by applying the following formula:

$$I_F = I_M 10^{(d\varepsilon_{exc}+s\varepsilon_{em})C_p/2} \quad (1)$$

which takes into account the detection geometry in FluoroMax4 equipment. In eq 1, I_F and I_M are respectively the true and measured emission curves, d and s are the path lengths of respectively excitation and emission light, and ε_{exc} and ε_{em} are the molar extinction coefficients at excitation and emission wavelengths. With this correction, emission spectra measured for $8.8 < C_p$ (μM) < 176 superimpose satisfactorily after normalization by the polymer concentration. In the following we will always plot emission spectra corrected for inner filter effects.

4. Photon Correlation Spectroscopy (PCS). Intensity−intensity correlation functions (ICFs) were measured at a fixed scattering angle θ = 90° with the ALV/DLS/SLS-5020F experimental setup (ALV Laser Vertriebsgesellschaft mbH, Langen, Germany), consisting in a He−Ne laser (22 mW, λ_0 = 632.8 nm), a compact ALV/CGS-8 goniometer system, and an ALV-5000/E multitau correlator. The incident wavelength lies well outside the absorption spectrum of the polymer so that no correction for absorption was necessary. Temperature was regulated to 25.2 ± 0.1 °C.

Samples were systematically filtered through 0.45 μm Millipore filters before PCS measurements. Furthermore, their UV−visible absorption was measured before and after filtration to estimate the amount of material retained on the membranes. Filtration did not affect significantly the sample concentration, except in the vicinity of R = 5.7 where the fraction of sample retained by the filter was about 0.5 (see the Supporting Information).

The normalized ICF $g^{(2)}(t)$ is related to the normalized correlation function of the scattered electric field $g^{(1)}(t)$ by Siegert's relationship, $g^{(2)}(t) = 1 + \gamma|g^{(1)}(t)|^2$, where γ is fixed by the detection geometry and is about 0.9 in our experiment. Due to the very low polymer concentration used in this study (C_p = 0.176 mM), experiments were performed in unusual conditions where the total intensity I_T scattered from the sample ($2.8 < I_T$ (kHz) < 15) was not always large compared to the one scattered from the buffer solvent ($I_{solv} \approx 1.5$ kHz). Therefore the apparent initial values of the ICF could decrease to values as low as 0.25, due to solvent contribution to the fluctuations of the total scattering intensity on characteristic time scales smaller than 1 μs and not measurable by the correlator.

The correlation functions of the scattered electric field $g^{(1)}(t)$ were analyzed with CONTIN software[74] to obtain the corresponding pseudodistributions of relaxation times $P(\tau)$ defined as

$$g^{(1)}(t) = \sum_i P(\tau_i) \exp(-t/\tau_i) \quad (2)$$

To estimate the influence of experimental noise on CONTIN output, for each sample 30 ICFs were measured overnight with an acquisition time of 600s for each one. Batch-processing of these data by CONTIN and subsequent statistical analysis of the outputs were done through CNTb, a set of scripts written for this purpose.[75]

5. Cryo-Transmission Electron Microscopy (cryo-TEM). Samples for cryo-TEM experiments were prepared following standard procedures on carbon-coated copper grids.[76] They were quenched in liquid ethane and brought to the Phillips CM12 microscope in a Gatan 626 cryogenic container. Images were recorded with SO163 films and digitized with Visilong Image Analysis software.

6. Isothermal Titration Calorimetry (ITC). We used the VP ITC (TA Instruments) to measure interaction isotherms during the titration of PTAA by DeTAB. Due to the sensitivity range of the apparatus (about 1 μJ per injected μL), more concentrated polymer solutions were used (C_p = 1.67 mM). To avoid the addition of surfactant titrant with concentration above the cmc, we have chosen DeTAB for these experiments. All solutions were prepared with

dx.doi.org/10.1021/la204862u | Langmuir 2012, 28, 4815−4828

buffered solvent (pH 9.7) and two titration solutions with surfactant concentrations 0.2 and 4 mM were injected with a 250 μL syringe equipped with a stirrer (250 rpm). The injected volumes were programmed to cover the range $10^{-3} < R < 1$. The two first injections for both surfactant solutions were not taken into account in the data analysis. All solutions were degassed 30 min under vacuum before use. The titration cell was regulated at 25 °C and the waiting time between each injection was 10 min. The heat associated with the dilution of the surfactant in the buffer was measured with the same conditions. This contribution was subtracted from the surface area of the peaks in the thermogram before calculating the molar heat associated with the interaction of PTAA and DeTAB.

RESULTS

1. Structure of PTAA/Surfactant Aggregates: PCS and cryo-TEM. Figure 1 shows the evolution of $P(\tau)$ as a function of the molar ratio of DoTAB to monomers. The data in Figure 1 correspond to CONTIN solutions obtained with the ensemble-averaged ICF calculated from the 30 individual measurements. These curves are less sensitive to the statistical noise in the data.[75]

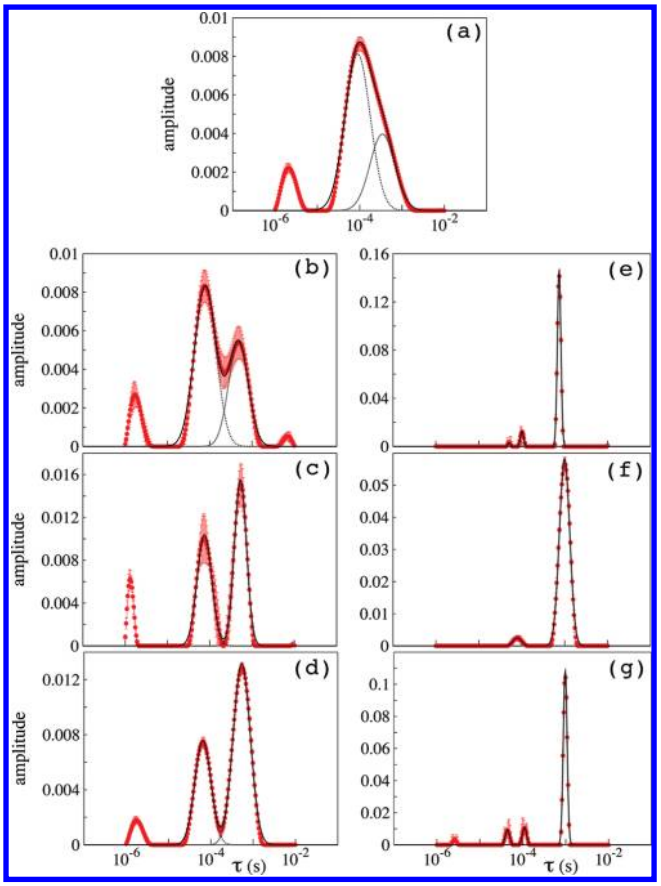

Figure 1. Distributions of relaxation times $P(\tau)$ obtained via CONTIN analysis for different values of the composition ratio R: (a) 0, (b) 5.7×10^{-4}, (c) 5.7×10^{-3}, (d) 5.7×10^{-2}, (e) 0.57, (f) 5.7, and (g) 57. The continuous lines are log-normal distributions fitted to the data.

A first peak appears at small relaxation times (<10 μs) and is due to fast fluctuation modes of the intensity associated with the solvent contribution. These fast modes are out of the range of the correlator board but contribute to the initial decay of the ICF. They appear at the lower limit of the range of relaxation times allowed for CONTIN analysis but the position of the corresponding peak has no real significance. As the total intensity I_T scattered by the sample increases, this contribution decreases and disappears for the samples with the largest I_T values (I_T > 10 kHz, 0.57 < R < 5.7).

For small and intermediate R values ($R \leq 0.57$), the curves $P(\tau)$ exhibit two peaks that are very close for R = 0 (pure polymer solution, Figure 1a) and separate progressively as R increases. In parallel their relative contributions to the total scattering intensity change, with the peak corresponding to the largest relaxation times becoming the largest contribution. For higher R values, these trends are pursuing: the contribution at large relaxation times becomes dominant and extremely narrow while the contribution of the one or two peaks at small relaxation times is very faint but reproducible on a large proportion (~2/3) of the 30 experimental runs. These contributions and their relative importance (with their associated error bars) can be ascertained only with the help of CNTb package,[75] after the $P(\tau)$ values have been fitted as a sum of log-normal distributions as shown in Figure 1, the contribution of each mode being given by its respective area S_i ($\sum_i S_i = 1$). The corresponding scattering intensities I_i can be calculated as $I_i = S_i (I_T - I_{solv})$.[77] The increase of I_T with composition ratio is linked to the similar behavior of I_L associated with the largest relaxation times, while the intensity I_S associated with the smaller relaxation times remains almost constant, about 1 kHz (see Supporting Information).

In this very dilute regime, the electrostatic interactions between chains are screened by the ionic strength of the buffer. Therefore the relaxation times can be safely associated with an effective hydrodynamic length characterizing the Brownian motion of the corresponding species. We estimate this length by using the Stokes−Einstein relationship to calculate the hydrodynamic radius of an equivalent hard sphere. Figure 2 shows the evolution of these radii with the composition ratio R.

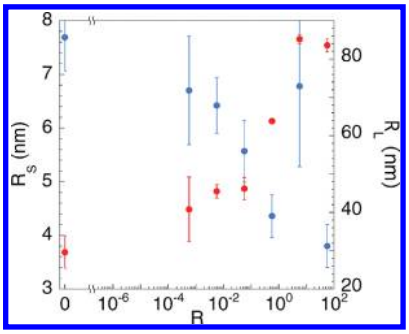

Figure 2. Evolution of equivalent hydrodynamic radii R_S (blue dots) and R_L (red dots) with the composition ratio R. Data are the mean values calculated on the results of $N \approx 25$ PCS runs. Errors bars correspond to the standard deviations on the set of N measurements. Therefore the standard errors on the means are smaller by a factor about 5 and the 95% confidence intervals on the means by a factor about 2.5 than the displayed error bars. See the Supporting Information for the reproducibility of the experiments.

The radii R_S and R_L, associated with the smaller and larger species, respectively, exhibit markedly different behaviors: over the range of composition ratio R_S decreases continuously, except for a jump at R = 5.7, from about 7 to about 4 nm, while R_L increases continuously from about 30 to about 80 nm. Thus the increase of the contribution of the larger objects to the scattering intensity is correlated with an increase in their effective hydrodynamic size. Using simple assumptions, it is possible to estimate the molar fraction of scattering units belonging to the small objects in the solution. Except in the

dx.doi.org/10.1021/la204862u | Langmuir 2012, 28, 4815−4828

vicinity of R = 1, it remains very close to 1 (see Supporting Information). Therefore, when the composition of the solution is very dissymmetric, i.e., for large excess of one of the constituents with respect to the other one, the large objects are rare, their strong contribution to the total scattering intensity is mainly due do their size, and most of the polymer chains and associated surfactants are found in the smaller objects.

Cryo-TEM results confirm this picture (Figure 3). For low R = 0.057, small and compact objects (∼5 nm) coexist with much larger ones (∼40−100 nm), but small objects are much more abundant (Figure 3, top). For R = 5.7, an unfiltered sample contains many more large objects with sizes up to 1000 nm (Figure 3, bottom). This explains why a large fraction of sample is retained by filter membrane for this particular composition ratio. Still a large fraction of the polymer chains is contained in large aggregates after filtration. It is then very difficult to measure the contribution of small objects (Figure 1e,f) by PCS (even after filtration) but they can be distinguished in the cryo-TEM image (Figure 3, bottom).

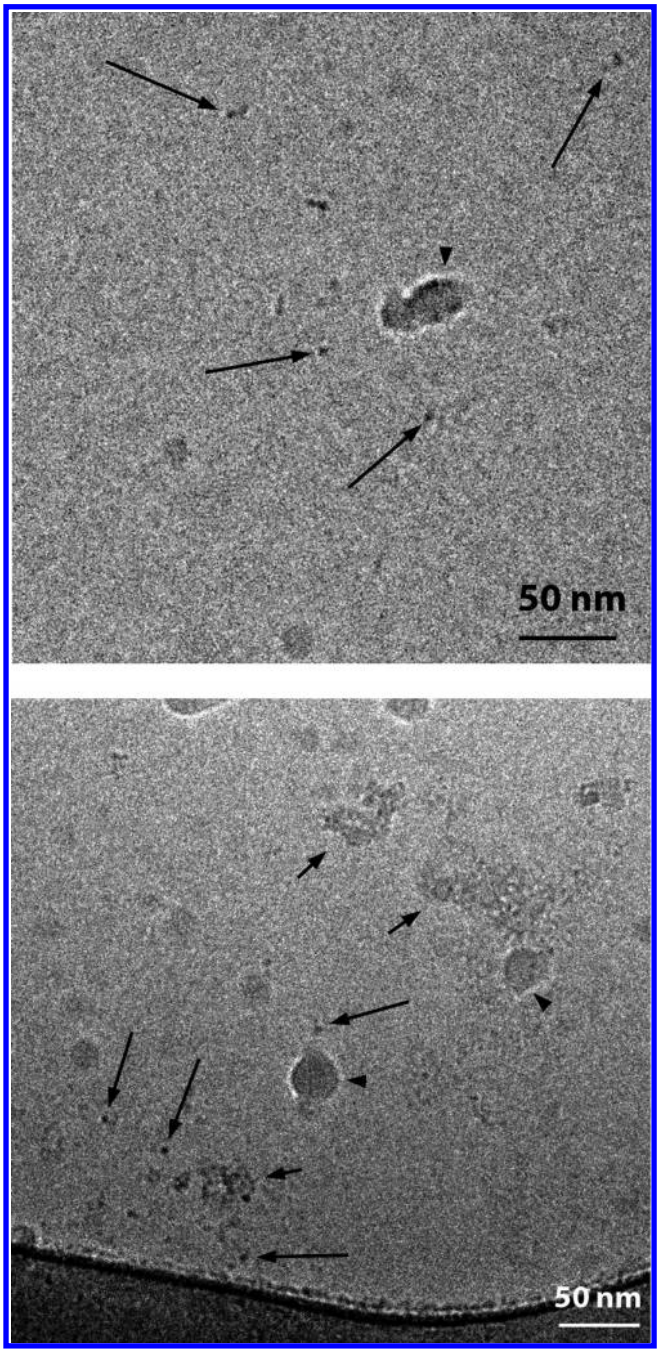

Figure 3. Cryo-TEM images obtained with unfiltrated DoTAB/PTAA samples: R = 0.057 (top) and 5.7 (bottom). Long and short arrows point to representative small (∼5 nm) and large (>40 nm) objects, respectively. Arrow heads point to ice contamination.

2. Optical Properties of PTAA/Surfactant Aggregates: Absorption and Emission Spectroscopies. Figure 4 shows the variation of the position λ_{abs} of maximum UV−visible absorption, measured in titration experiments, as a function of composition ratio R for different surfactant lengths n. In Figure 4a, we used our standard conditions (C_p = 0.176 mM, pH 9.7, ionic strength 36 mM) while data in Figure 4b correspond to higher polymer concentration and ionic strength conditions (C_p = 0.68 mM, pH 9.3, ionic strength 48 mM). The λ_{abs} values for the pure polymer solutions (R = 0) in the two conditions differ by about 20 nm, mainly because of the differences in ionic strengths. Indeed at large pH, λ_{abs} has been observed to increase with the ionic strength.[78] At fixed C_p, some systematic small fluctuations (±2 nm) in the initial values of λ_{abs} are also observed (R = 0). They are likely due to small variations in the experimental conditions (atmospheric pressure, hygrometric saturation, Ar flux) that affect the amount of carbonic acid present in the sample. These fluctuations are much larger than the experimental error on λ_{abs} determination (±0.2 nm) allowed by the parabolic fit of the maximum. They explain the much better precision on $\lambda_{abs}(R)$ curves measured in situ by titration experiments in comparison with values measured in standard cells on individual samples prepared at a given R. Apart from these differences in the initial value of λ_{abs}, the two sets of curves display the same qualitative behavior and three different regimes can be distinguished.

For very small R values, typically from R = 0 up to about 10^{-3} (regime I), there is a very small decrease of λ_{abs} of the order of 2 nm. This decrease would not be detected with individual samples prepared and measured at a given R value in standard cells, due to the experimental errors mentioned above. There is no clear trend in the value of the slope associated with this decrease, e.g., with the length of the alkyl chains. We cannot totally exclude some contamination by atmospheric CO_2 despite the Ar flux in the titrated solution. Indeed we observed a decrease of λ_{abs} by about 10 nm after a few days for a pure polymer solution conserved in a sealed Hellma cell. This decrease is faster when the polymer concentration is lower and is not observed for polymer solutions at pH 5.3 (collapsed state). Therefore although the pH is kept constant by the buffer, it seems that progressive contamination by CO_2 shifts the acido-basic equilibrium in the medium and affects the neutralization degree of the polymer chains and their absorption spectra. In the titration experiments, this first regime up to $R \approx 10^{-3}$ corresponds to a titration duration of at most 100 min and this possible contamination has only a minimal effect.

A second regime (II) is linked with an abrupt decrease of λ_{abs} by 30−50 nm, which occurs on one or two decades of R increase and becomes steeper for n values increasing from 6 to 12. For even larger n values (n = 14 and 16) the steepness of the decrease does not seem to change any more.

A third regime (III) occurs only for surfactant length larger than n = 10 and corresponds to a slight increase of λ_{abs} followed by a jump for R values in the range 1−10, depending on n.

dx.doi.org/10.1021/la204862u | Langmuir 2012, 28, 4815−4828

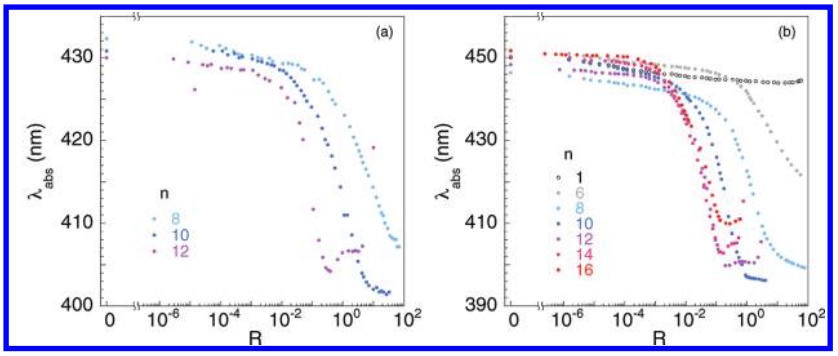

Figure 4. Variation of the position of maximum absorbance λ_{abs} with the composition ratio R for different alkyl chain lengths n: (a) C_p = 0.176 mM and (b) C_p = 0.68 mM. Data are obtained by in situ measurements during titration.

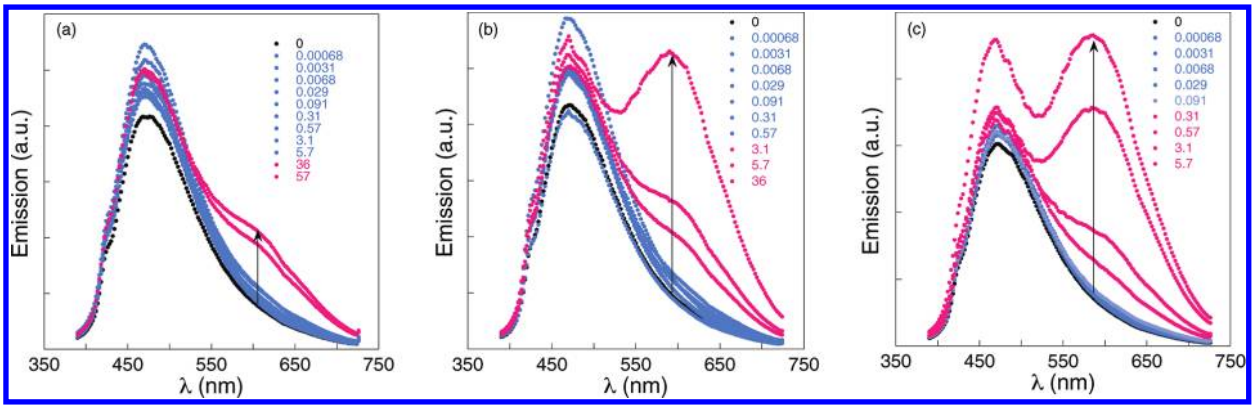

Figure 5. Effect of surfactant addition on the emission curves for different surfactant tail lengths: (a) OTAB, (b) DeTAB, and (c) DoTAB. The numbers in the legends correspond to composition ratio values R. The black curves are the emission spectra of pure polymer (C_p = 0.176 mM). The blue and red colors help to distinguish the R values beyond which a second emission band around 600 nm appears. The samples are not filtered.

This general behavior is completely different from that observed with tetramethylammonium bromide (n = 1), where regimes II and III are absent (Figure 4b). Therefore it is related to the presence of an hydrophobic tail in the surfactants. As a general trend, the increase of the surfactant hydrophobicity shifts the onset of the three regimes to lower R values. For $6 \leq n \leq 12$, the regime II shifts to smaller R range when n increases. For $10 \leq n \leq 16$, this trend disappears progressively but the minimal value of λ_{abs} increases at a roughly constant value $R_{min} \approx 0.15$ and the jump in λ_{abs} occurs at decreasing R values.

Figure 5 displays the evolution of emission spectra for complexes made from OTAB, DeTAB and DoTAB (C_p = 0.176 mM, pH 9.7, ionic strength 36 mM). For comparison, the emission spectrum of the pure polymer solution is also shown: it is a broad peak with a maximum at $\lambda_{em} \approx 472$ nm (black curve). The blue labeling turns to red to emphasize the R values where the emission curves display a striking transformation. In the case of DoTAB surfactant (Figure 5c), this occurs for R values in the vicinity of R_{min}. Below R_{min}, the emission spectra are almost insensitive to the presence of surfactant. Above R_{min}, a shoulder appears in the emission spectra at larger wavelengths and turns progressively into a second emission peak around 600 nm as R increases. Thus the strongest effects of surfactant binding appear in the emission spectra above R_{min}, i.e., when the absorption spectra become much less sensitive to the further addition of surfactant. Although R_{min} cannot be defined for shorter surfactants (n = 8, 10), a similar shoulder appears in the presence of OTAB and DeTAB only for R values where λ_{abs} has considerably decreased (Figure 5a,b). Therefore, for all three surfactants, it seems that the second emission band can occur only after the large decrease in λ_{abs}.

In order to quantify all of these observations, we analyzed the full emission profiles as a combination of two contributions. We first evaluated the second emission band by subtracting an average spectrum calculated from those recorded at lowest R values (blue curves). The resulting curves can be satisfactorily described by a Gaussian curve with maximum location and width only weakly dependent on the surfactant length. We finally extracted the amplitude of the different contributions for each surfactant over the whole R values. If the shape of the second contribution is very similar for each surfactant, both its onset and its amplitude depend markedly on the surfactant length. It appears sooner and exhibits a much steeper growth when n = 12 (see the Supporting Information).

For the sake of comparison we show in Figure 6 the absorption and emission spectra for solutions of complexes at a higher composition ratio, R = 57. For complexes formed with DoTAB the second emission peak is very intense, about 3 times brighter than the initial emission peak of the pure polymer, which has disappeared. By contrast, the second emission band is still weak for complexes made from OTAB, much less intense than the emission of the pure polymer. Complexes formed with DeTAB have intermediate behavior.

In Figure 6 are also shown the absorption and emission curves of the same samples after filtration. The absorption curves show very little effect of the filtration in agreement with the data reported for PTAA/DoTAB complexes (Figure S2). On the other hand the emission curves display a much more contrasted behavior according to the surfactant length. For

dx.doi.org/10.1021/la204862u | Langmuir 2012, 28, 4815−4828

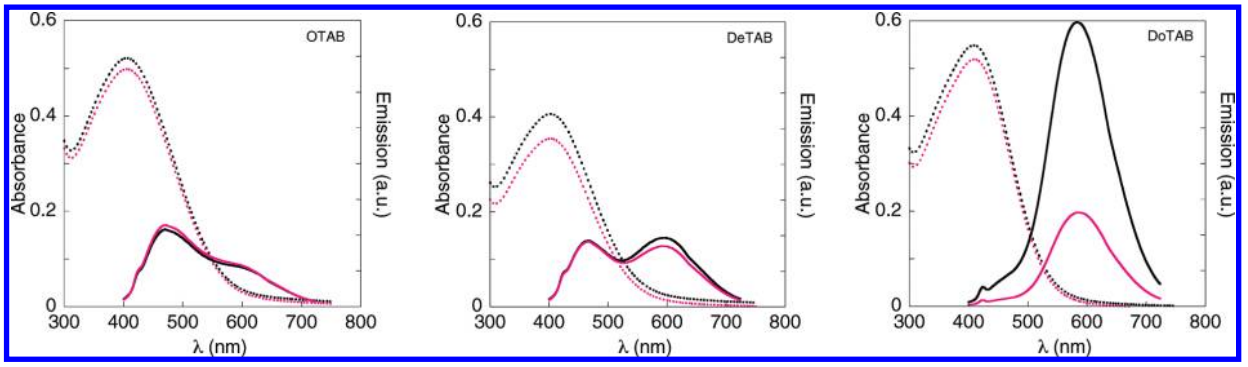

Figure 6. Absorption (dotted lines) and emission (continuous lines) spectra at fixed composition ratio R = 57 (C_p = 0.176 mM) for the three surfactants OTAB, DeTAB, and DoTAB. Black and red colors refer to spectra measured, respectively, before and after filtration of the samples.

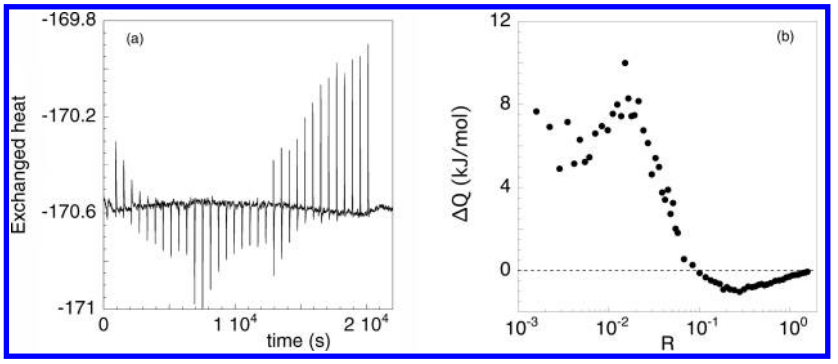

Figure 7. Thermogram (a) and differential enthalpy curve (b) during the isothermal titration of PTAA by DeTAB (C_p = 1.67 mM). Endothermic processes correspond to down spikes in (a) and to negative ΔQ in (b). The thermogram in (a) corresponds to the injection of the most concentrated surfactant solution for $R \geq 0.061$.

OTAB based complexes, the filtration has no effect on the two bands of the emission curve, while the emission by DoTAB-based complexes is very sensitive to the filtration: the amplitude of the second emission band decreases by a factor about 3 despite the low sample fraction retained in the filter. Complexes formed with DeTAB show an intermediate behavior with a small effect of filtration on the second emission band and no effect on the emission of the pure polymer.

3. Thermodynamic Aspects of PTAA/Surfactant Binding: Isothermal Titration Calorimetry. Figure 7 displays the thermogram and the differential enthalpy curve $\Delta Q(R)$ measured when DeTAB is progressively added to a buffered solution of PTAA at a concentration C_P = 1.67 mM, about ten times larger than for the previous results, as explained in the experimental section.

The thermogram displays two distinct regimes corresponding to exothermic and endothermic heat exchanges upon addition of surfactant (Figure 7a). The differential enthalpy curve (Figure 7b) is calculated from the areas of the peaks in Figure 7a, corrected from the contribution of the dilution of the surfactant and normalized by the amount of added surfactant. The general aspect of the curve $\Delta Q(R)$ agrees with usual interaction isotherms of oppositively charged surfactant/polyelectrolyte mixtures.[79] At small R values (R < 0.006), the isotherm exhibits a plateau behavior at about 6 kJ/mol, which corresponds to a noncooperative exothermic binding of the surfactant molecules to the polymer. Experimental errors are larger in this region since the injected surfactant quantities are correspondingly small. Then the exchanged heat increases to a maximum of about 8 kJ/mol for $R \approx 0.015$. This rise corresponds to the onset of cooperative binding where the presence of bound surfactants facilitates further binding. Then there is an abrupt decrease to 0 at $R \approx 0.1$ where the exchanged heat becomes negative, indicating a new endothermic binding process that can occur for entropic reasons. Finally this negative ΔQ vanishes smoothly for $R \approx 1$. We did not pursue the experiments above this value because the injected surfactant solutions would have contained surfactant micelles.

■ DISCUSSION

Previous small-angle scattering results[63] on more concentrated systems have shown that salt-free semidilute solutions of fully neutralized PTAA display the classical behavior of semidilute polyelectrolyte solutions: they exhibit the usual correlation peak with a position that scales like $C_p^{1/2}$ and an upturn at low scattering vector that is due to a small fraction of aggregates. Thus in dilute solutions we can safely assume that the same chains are molecularly dispersed since the most abundant species exhibits a very reasonable size (R_S = 7.7 ± 0.7 nm) for the apparent hydrodynamic radius of an isolated chain (Figure 1a). The weak shoulder on large relaxation times side, which we resolved as a second log-normal distribution, is then likely a trace of the chain aggregates responsible for the upturn in SANS intensity at higher polymer concentations.[63] The fact that our CPE chains are mostly molecularly dispersed in the solution has consequences on their solution behavior upon surfactant binding.

Binding by DoTAB. Combining the various information gathered by PCS and spectroscopy experiments, we obtain a rather clear picture of the effect of DoTAB binding on the CPE chains, based on well-established behavior of oppositely charged polyelectrolyte/surfactant mixtures.[15−38]

dx.doi.org/10.1021/la204862u | Langmuir 2012, 28, 4815−4828

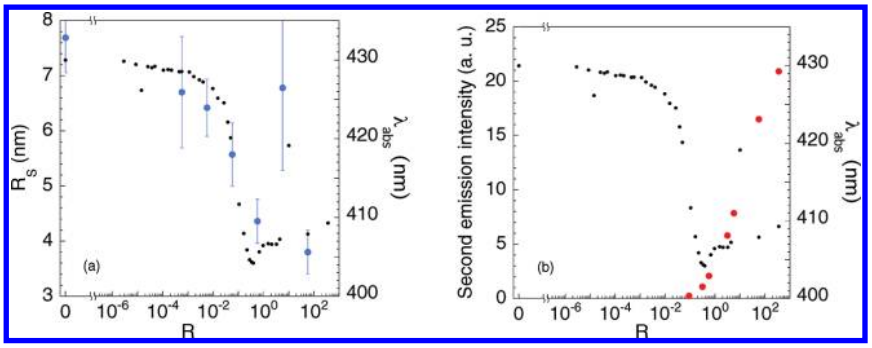

Figure 8. Parallel evolutions of (a) R_S (blue dots) and λ_{abs} (black dots) and (b) the intensity of second emission band (red dots) and λ_{abs} (black dots), as a function of composition ratio R (DoTAB, C_p = 0.176 mM).

For small composition ratio, the exchange of condensed Na counterions by oppositely charged alkyl chains is favored by entropic and enthalpic gains and the binding of the free charged surfactant with the oppositely charged chains follows spontaneously. Thus increased hydrophobic interactions inside the coils induce their progressive collapse as the amount of added surfactant increases and the apparent hydrodynamic radius of the dispersed chains decreases by a factor close to 2 for composition ratios well below 1 (Figure 2).

Further surfactant addition enriches the mixed aggregates until combined effects of charge neutralization and increased hydrophobicity yield complexes with a very poor solubility. In more concentrated solutions, precipitation would occur but in our very dilute solutions, this phase separation is prevented, at least on the time scale of our experiments. Instead very slow formation of superaggregates occurs and appears as a surge in the amount of sample eliminated by filtration, a large increase in the scattering intensity of the filtered solutions, and an increase in the volume fraction of the larger objects still present after filtration (see corresponding figures in the Supporting Information). The size of these large objects also increases (Figure 2). Cryo-TEM images show distinctly the coexistence of very small dense mixed aggregates (~5 nm) and superaggregates (>40 nm) in the unfiltered solution (Figure 3, bottom).

For large excess of added surfactant (R > 10), the superaggregates get enriched in surfactant and gain a net charge that favors their redissolution: they break and the fraction of sample that can flow through the filter increases back to 1 and the total scattering intensity decreases (see Supporting Information). In the filtered solution, the average size R_L of superaggregates tends to saturate (Figure 2).

This behavior and its interpretation are quite well established for mixtures of ionic surfactants and oppositely charged polyelectrolytes with a saturated backbone. As far as we know, these features were never observed before in the case of CPEs. In the relevant literature, surfactants are usually added to dissolve preexisting aggregates of poorly soluble chains. The so-called surfactochromicity is then mainly associated with the dissociation of chain aggregates existing at R = 0.[39,40,42−54,57] Here the good water solubility of PTAA chains yields a specific spectroscopic behavior upon DoTAB addition.

For small composition ratios, R < 1, chain collapse is associated with an increase of the conformational disorder and a decrease of the average conjugation length signaled by a blue shift of the absorption spectra (Figure 8a). As far as we know, such a direct correlation is evidenced here for the first time for CPEs. Strikingly the emission spectra are nearly insensitive to the individual chain collapse (Figure 5c). In contrast with results reported for other conjugated backbones, no significant emission intensification[39,40,42,44,46−50,56,57] or quenching[43,51−54,56,57] can be observed for these small composition ratios. We found also that the emission spectrum of the pure PTAA solution is much less sensitive to pH value than its absorption spectrum (see the Supporting Information). Both behaviors support the explanation of an energy transfer to chromophores with lower energies after the excitation,[65−70] which we mentioned above to explain the effect of excitation energy on the emission spectra.

On the other hand, after chain collapse, the enrichment of the mixed polymer−surfactant aggregates with new surfactant molecules is associated with the surge of a new emission band red-shifted by nearly 130 nm with respect to the initial emission band of the pure polymer (Figures 5c and 8b). The latter disappears progressively as the intensity of the new emission band increases. In this regime the absorption spectra are much less sensitive to the enrichment of the mixed aggregates by surfactant molecules except in the vicinity of $R \approx 5.7$ where the fraction of sample retained by the filter is highest.

In Figure 8 we added data points corresponding to a sample first prepared at R = 57 and then enriched at R = 360. For this last value the surfactant concentration in the solution is very high and about five times the cmc. For these two samples, the positions of the absorption maximum, λ_{abs} = 407.9 (R = 57) and λ_{abs} = 409.3 (R = 360), do not differ significantly from the values measured below R = 5.7. The emission maximum is slightly blue-shifted, λ_{em} = 586.7 nm (R = 57) and λ_{em} = 583.0 nm (R = 360), compared to $\lambda_{em} \approx$ 600 nm at smaller R values. However its intensity is still steadily increasing. The slight blue shift and the steady emission increase at high composition ratio are consistent with the chain environment becoming less and less polar as the aggregates are further enriched with surfactant.[51]

The appearance of a new emission band at about 600 nm is thus the signature of a new structure for the mixed surfactant/CPE aggregates at high composition ratio. Indeed surfactant−polyelectrolyte complexes formed at high composition ratio in dilute solutions have a structure similar to the mesophases observed at higher polymer concentrations.[80−84] The large red-shift compared to the initial emission peak of the pure polymer suggests that excimer formation is facilitated by this new structure. It is worthwhile noticing that chain collapse upon pH decrease does not modify the shape of the emission curve. Therefore the intimate mixing of the surfactant molecules with the CPE chains is required to observe the second emission band.

dx.doi.org/10.1021/la204862u | Langmuir 2012, 28, 4815−4828

Influence of Alkyl Chain Length. The effects of varying the alkyl chain length in the surfactant molecules are consistent with the above picture and bring complementary informations. The evolution of λ_{abs} with R shows that the collapse of the chains is delayed to higher R values as n decreases from 12 to 6. This shift is no surprise since it is related to a similar shift of the critical aggregation concentration (cac) that is well documented in the literature.[16−18,21,32] For $n > 12$, the behavior is more complex since the collapse does no longer shift to smaller R values as n increases. Also the minimal value of λ_{abs} increases (Figure 4), which suggests that the steric constraints associated with the bound surfactants start to swell the collapsed chains.

On the other hand it appears increasingly difficult to observe a full chain collapse as n decreases. The highest composition ratios investigated for OTAB and HTAB are between 10 and 100, depending on the polymer concentration, and the solution contains then a large excess of isolated surfactant molecules available for binding. However further surfactant addition has still an effect on the chain conformation and λ_{abs} has not reached a steady state value for these large composition ratios. This means that the mixed aggregates are not yet saturated with surfactant at these R values. The balance between the enthalpic gain and the entropic penalty associated with the surfactant binding is likely responsible for these effects. Since the entropic penalty depends on the surfactant concentration in the solution and the chain collapse is linked to the local surfactant concentration inside the mixed aggregates, the binding fraction and the chain collapse result from a complex interplay between the surfactant hydrophobicity and the polymer concentration in the solution.

Finally we note that the surfactant HTAB ($n = 6$) has no known cmc value and is not forming measurable micelles when mixed with poly(styrene sulfonate).[85] This points to a significant contribution of the strong hydrophobicity of PTAA backbone toward the formation of mixed polymer−surfactant aggregates. Molecular simulations of gemini cationic surfactants bound to a PFP-based polyanion have shown similar strong interactions of the alkyl chains with the polymer backbone.[54] Moreover surfactochromicity was also described for CPEs mixed with neutral or like-charged surfactants, which shows the significant role of nonCoulombic interactions in the binding of surfactants to CPEs.[52] A strong attractive interaction between polymer backbone and surfactant is expected to decrease the influence of hydrophobic interactions between surfactants and the related cooperativity effects in the binding process.[15,27,28]

The emission properties of the complexes are also influenced by the alkyl chain length, with two main effects as n decreases from 12 to 8: the appearance of the second emission band is delayed to larger R values and its growth is slower (see Supporting Information). These features can be explained by the same effects as discussed above for the evolution of $\lambda_{abs}(R)$ with n.

Samples prepared at same composition ratio $R = 57$ with OTAB, DeTAB, and DoTAB, are in fact very different, both in their dispersion state and their spectroscopic properties (Figure 6, black curves). With DoTAB, the light scattering intensity has started to decrease after having reached its maximum at $R \approx 5.7$ and the larger superaggregates undergo already a redissolution process. With OTAB, the collapse of the chains is still not complete at the same R value (Figure 4). With DeTAB, we have an intermediate situation where λ_{abs} values start to initiate a plateau for the highest R values. Thus the same composition ratio corresponds to different internal structures in the three systems, which do not exhibit the same emission features. The full collapse of the chains at small R values seems a necessary condition to observe an intense second emission band at larger R values.

The filtration of the same samples (Figure 6, red curves) shows that the amount of material retained on the filter is quite comparable, about 5, 15 and 7% for respectively OTAB, DeTAB, and DoTAB. This quite low retention has however a dramatic effect on the second emission intensity, which decreases by a factor about 3 after the filtration in the case of DoTAB-bound aggregates. This shows that there is a large fraction of red emitters in the material that is filtered out. On the other hand, the emission intensity increases steadily with DoTAB addition, even above the cmc (Figure 8), and this suggests that this intensity is not linked to the size of the larger superaggregates, which is expected to decrease with the amount of added surfactant.

Therefore it seems that a hierarchical structural model could account for our experimental results. The basic unit would be the mixed surfactant/CPE with size ∼5 nm formed at small R values but the second emission band would appear only upon aggregation of these units after their enrichment in surfactant at large composition ratios, probably through the formation of excimers. The structure of these basic units depends on the hydrophobicity of the surfactants and seems an important ingredient. After filtration, the persistence of the second emission band together with the existence of objects with very well-defined size $R_L \approx 80$ nm (Figure 1g) indicates that these nanometric aggregates are responsible for the new emission. However, in the unfiltrated sample, a large fraction of these nanoparticles are aggregated in much larger flocs that can be filtered out. In this picture the disappearance of the initial emission of the pure polymer would be due to its progressive replacement by the excimer emission as the nanometric aggregates are forming.

Critical Aggregation Concentration. The critical aggregation concentration can be associated with the onset of chain collapse.[27,28,35] Therefore the correlation of the decreases in R_S and λ_{abs} should provide us with a convenient determination for the cac in surfactant/CPE mixtures. Here we can tentatively associate the cac with two easily determined characteristics of the curves $\lambda_{abs}(R)$ in Figure 4, either their departure from regime I, i.e., the onset of regime II, or the intersect of two straight lines fitted in regime I and in regime II (see Supporting Information). Figure 9 shows the dependence on n of these cac values together with the cmc values of the pure surfactants in pure water and brine (0.1 M NaCl).[85−87] Clearly the general behavior of these cac values as a function of alkyl chain length does not depend on the method used to determine them. There is however a factor about 10 between the numerical values obtained with the two methods.

For saturated polyelectrolytes, the representation in Figure 9 yields slopes associated with the energy ψ saved by bringing one CH_2 unit from water to a less polar environment, $C_{cac} \approx \exp(-\alpha n\psi/kT)$,[16,17,26,32] and a simple model[26] predicts that the coefficient α should be identical for the variations with n of the cac and the cmc in brine. The data in Figure 9 do not show the expected exponential dependence over the whole range of n values: the cac values estimated for TTAB and CTAB deviate from a linear extrapolation of log(cac) measured for surfactants with smaller alkyl chains. Therefore it is difficult to conclude on a comparison of slope values.

dx.doi.org/10.1021/la204862u | Langmuir 2012, 28, 4815−4828

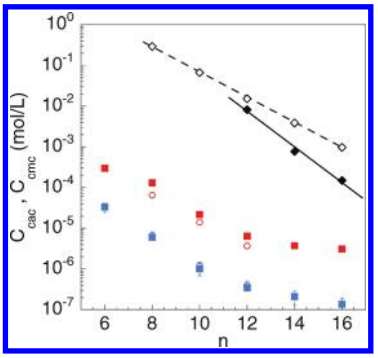

Figure 9. Variation of the cac with the alkyl chain length n: C_p = 0.176 mM (circles); C_p = 0.68 mM (squares). Blue labeled data are obtained from the departure of regime I, red labeled data from the intersection of two straight lines drawn in regimes I and II (see the Supporting Information). Data and error bars are mean values estimated from several titrations. The literature values[85−87] for the cmc of the surfactants in pure water (opened diamonds) and in 0.1 M NaCl brine (closed diamonds) are also plotted for comparison.

The cac values are, depending on the method used to determine them, about four to 5 orders of magnitude smaller than the cmc of the pure surfactants. For similar polymer concentration and ionic strength, DoTAB has a cac about 0.1 mM with dextrane sulfate and about 0.01 mM with polystyrene sulfonate, a difference attributed to the hydrophobicity of polystyrene backbone.[15] In the case of DoTAB/PTAA, we estimate a cac about 0.4−5 μM, below the value obtained with polystyrene sulfonate by a factor 2−20. The very small ratio cac/cmc is an additional argument for a very strong interaction between the surfactants and the hydrophobic conjugated backbone.[27,28] In this case, it is expected that a much more progressive chain collapse takes place on a wider interval of surfactant concentrations. It becomes then more difficult to define accurately a cac.[27,28] In these conditions, it can be expected that our data do not follow the prediction of a simple model, which does not consider explicitly the interactions between surfactants and hydrophobic backbones to derive the cac dependence on hydrophobic tail length.[26]

We can estimate the average number of bound surfactant molecules per chain corresponding to our cac values. In the case of DoTAB, it corresponds to about 0.7−7 (respectively 0.2−2) surfactant/chain for C_p = 0.176 mM (respectively C_p = 0.68 mM). These numbers are very small, but, as emphasized by one referee: "The cac is the surfactant concentration where micelles first can be detected and at this point the concentration of micelles (and therefore the concentration of micellized surfactant) can be extremely low. Thus, it is problematic to make statements about the number determined here. The number of surfactant monomers bound to the polyion just below the cac need not be directly related to cac, and can in principle be close to zero, i.e., the surfactant binding may practically coincide with cac". In the present case, the absorbance spectra are clearly blue-shifted around these tentative cac values, which supports a progressive effective binding of the surfactant monomers to the chains and suggests an alternative explanation: the decrease in $\lambda_{abs}(R)$ might reflect mainly a decrease of the average conjugation length, each bound surfactant acting as a random boundary to the delocalization of π electrons. This would imply that the cac cannot be easily deduced from the variation of $\lambda_{abs}(R)$. Although PCS results show a good correlation between the decrease in $\lambda_{abs}(R)$ and R_S (Figure 8a), the experimental errors on the latter values prevent their use to assign the cac value. Therefore another technique is needed to confirm the location of the cac on the $\lambda_{abs}(R)$ curves.

Considering this strong hydrophobicity of PTAA backbone, we can anticipate that cac determination by measuring binding isotherms with surfactant-selective electrodes would be as difficult for PTAA/surfactant system as it is indeed for other hydrophobic polymer/surfactants associations.[19,88]

Isothermal titration calorimetry provides an alternative method for this purpose[31,89−91] since the rise in the differential enthalpy curve (Figure 7b) can be associated with the onset of cooperative binding and the location of the cac. The value $C_{cac} \approx 15$ μM at a polymer concentration C_p = 1.67 mM can be compared with the values obtained from the absorption measurements with DeTAB, $C_{cac} \approx 1-14$ μM at C_p = 0.176 mM and $C_{cac} \approx 1-22$ μM at C_p = 0.68 mM. The concentrations, ionic strength and pH conditions are not homogeneous for these scarce data and it is only possible to conclude that cac values estimated from absorption spectroscopy and ITC have the same order of magnitude. This confirms a small value about a few unities for the average number of bound surfactant per chain at the cac. Systematic comparisons between the cac values measured by the two techniques need clearly to be done. They are postponed to future work because they require the synthesis of a new sample batch due to the higher concentrations needed for combined ITC and absorption spectroscopy experiments.

As a final comment, we note that the average aggregation number of the micelles should remain about the same in the presence and in the absence of the polyions.[22−24,29] Considering the numbers associated with our experimental conditions, this implies here an inhomogeneous binding process, some chains being dressed and collapsed while others remain free of bound surfactant. Such inhomogeneous binding was observed in the case of DNA/CTAB mixtures[92,93] and predicted by some models.[24,34,94] It could justify the presence of different small size species in the time distribution functions obtained in the PCS experiments (Figure 1e,g).

To summarize, it appears that the present system does not exhibit a cac in the usual meaning of the term where the associated collapse transition is rather sharp. Here the correlated decreases in R_S and λ_{abs} occur in a rather wide range of composition ratio and the binding of surfactant to the hydrophobic backbone is likely inhomogeneous. Therefore both R_S and λ_{abs} are averaged quantities measured on an assembly of chains with different conformations. Thus the strong hydrophobicity of the backbone appears as an essential feature to design sensitive and quantitative colorimetric sensors for ligands with hydrophobic domains.

Binding Processes. Another interesting feature revealed by the ITC experiments is the existence of two different processes in the binding of DeTAB to PTAA. The first exothermic process at low R values shows that both the initial non-cooperative binding and the cooperative binding (above the cac) are enthalpically favored. This is in agreement with our comments above concerning the role of the hydrophobicity of the PTAA backbone in the binding process. In fact the binding between oppositely charged surfactants and hydrophilic polyelectrolytes is often endothermic and is favored only because of entropic reasons.[30,31,33,90] On the other hand when the polymer backbone is hydrophobic, the initial binding is exothermic.[90] A transition between endothermic and exothermic behavior has also been observed upon decreasing the

dx.doi.org/10.1021/la204862u | Langmuir 2012, 28, 4815−4828

charge density of the polymer backbone.[31,33] At higher composition ratios, the intrachain micellization of bound surfactants has been associated with an endothermic contribution.[30] A similar mechanism could explain the occurrence of endothermic behavior in our case as the mixed aggregates are progressively enriched with bound surfactants after the hydrophobic backbone has been covered in the initial steps. Further detailed study is needed to confirm this as yet tentative explanation.

Comparison with Other Systems. The appearance of a new emission band upon addition of surfactants to conjugated polyelectrolytes has been observed previously in only two studies as far as we know. The first example is a weakly soluble anionic oligomer (DP = 9) based on a PFP backbone (PBS-PFP) interacting with CTAB.[51] The oligomer solution is very dilute (8.6 μM) and the stoichiometry ratio varies between about 0.04 and 4.5. The authors observe a decrease of the emission peak centered around 424 nm until $R \approx 0.5$ where a new emission band centered about 525 nm appears. Meanwhile the initial emission peak shifts slightly to the blue at 418 nm. These phenomena are attributed to an increase in the interaction between the oligomers upon surfactant addition, which would favor energy transfer to lowest energy states associated with aggregates or excimers, the slight blue shift being due to the local environment of the oligomers becoming less polar.

The second example is a cationic polyelectrolyte based on a PPV backbone (TEAO-PPV) interacting with sodium dodecyl sulfate surfactant.[44] The polymer concentration is low (20 μM) and R varies between 0.05 and 1000. The very broad initial fluorescence peak is centered at about 520 nm. It shifts to 535 nm and its intensity increases by a factor 2 when R increases to 0.5. Then as R is increased to about 50, this initial fluorescence vanishes and is replaced by a less intense emission centered around 585 nm. Above R = 250, the initial fluorescence reappears and dominates the second emission band that does not disappear. In parallel the position of the absorption maximum shifts from 445 to 483 nm ($0.05 < R < 5$) then back to 465 nm (R = 1000). These observations are interpreted in relation with the cac and the cmc of the system. Above the cac, the first exchange between counterions and surfactants relax the torsion of the backbone due to the electrostatic interactions and favor a more planar conformation, associated with a red shift of λ_{abs} and increased interchain interactions that favor the formation of excimers with lower emission energies. Then, above the cmc of the surfactant, the polymer chains adsorb onto the surfactant micelles and the induced constraints on the backbone decrease the average conjugation length resulting in a blue shift of the absorption spectra. As surfactant molecules intercalate between the chains, the decreased interactions between the chains are less favorable to excimer formation and the initial emission behavior tends to be recovered.

Thus, our system displays a third scenario where, upon surfactant addition, the collapse of the individual chains is the first step. For long enough alkyl chain length, they fold then in a new conformation that favors the appearance of a very intense second emission peak upon aggregation of these basic units at large composition ratios.

CONCLUSIONS

Upon binding by cationic surfactants, the conjugated polyanion PTAA exhibits original spectroscopic properties in comparison with other conjugated polyelectrolytes, due to its good water solubility. In particular absorption and emission spectra show markedly opposite sensitivity to the presence of bound surfactants in the two regimes of composition ratio R, $R < 1$ and $R > 1$.

For small R values, the UV−visible absorption of the solutions is highly sensitive to the presence of minute amounts of bound surfactants and the maximum absorption position λ_{abs} shifts to shorter wavelengths by 30−50 nm as the apparent hydrodynamic radius of the chains R_S decreases by a factor 2. Thus conformational rearrangements during the chain collapse are associated with a large decrease of the average conjugation length. Emission curves in this R range are essentially insensitive to the collapse of the chains and the presence of bound surfactants, likely due to excitation energy transfer to remaining longer chromophores.

For large R values, the absorption curves are only weakly sensitive to changes in the composition ratio while the emission spectra display a new emission band shifted to larger wavelengths by nearly 130 nm. The intensity of this new emission band increases with the amount of added surfactant, until it becomes more intense than the initial fluorescence of the pure PTAA and the latter vanishes (DOTAB). We interpret these features as the signature of the formation of new structures, as the mixed surfactant/polymer aggregates get enriched in surfactant and form superaggregates at large R values. The internal organization of these new structures remains an open question but it could be similar to those reported for other surfactant/polyelectrolyte aggregates.[80−84]

As the surfactant tail becomes shorter, the blue shift of λ_{abs} and the intensity rise of the new emission are delayed to larger composition ratios while their variations become smoother functions of the surfactant concentration. As yet we cannot conclude whether the lower surfactant hydrophobicity has a direct effect on the chain conformation and the internal organization of the new stuctures, or merely results in a lower ratio of bound to free surfactant at a given surfactant concentration. Most likely, both effects are intertwined.

The strong hydrophobicity of the conjugated backbone plays a very important role. In particular, the effects of bound surfactant can be measured for very small average number of bound surfactant per chain, at composition ratios much lower than in any previously studied mixtures of oppositely charged surfactants and polyelectrolytes. This suggests an inhomogeneous binding of the surfactants to the chains at small R values. Another consequence of this strong hydrophobicity is to blur the notion of cac, and to smooth the collapse transition and therefore the decrease of $\lambda_{abs}(R)$.

The particular spectroscopic properties of the PTAA sample investigated here seem related to its unique combination of a strongly hydrophobic backbone, a large ratio of contour length to persistence length, and an overall good aqueous solubility. Our results show that a conjugated polyelectrolyte with these characteristics is well suited as a quantitative colorimetric biosensor at small composition ratio, and as a fluorescent biomarker at large composition ratio.

ASSOCIATED CONTENT

Supporting Information

Details and figures on the following: the error made on the maximum absorption position, the influence of excitation energy on the emission characteristics, the effect of filtration on sample concentration, the evolution of the scattering intensity with composition ratio, the relative abundance of small and large objects, the analysis of the second emission band, the

influence of pH on spectroscopic properties, the determination of cac values, raw ITC data, and the reproducibility of PCS results. This material is available free of charge via the Internet at http://pubs.acs.org.

AUTHOR INFORMATION

Present Address

[†]Institut Laue Langevin, 6 rue Jules Horowitz, BP 156, 38042 Grenoble Cedex 9, France.

Notes

The authors declare no competing financial interest.

ACKNOWLEDGMENTS

A special thank is due to Dr. M. Rawiso who initiated studies on conjugated polyelectolytes in Institut Charles Sadron. We are grateful to him for many enlightening discussions about the links between the conformation and the spectroscopic properties of conjugated polymers. It is a pleasure to thank Drs. M. Duval and J. Selb for their help and insightful comments concerning PCS and optical spectroscopy measurements, respectively. The work by Dr. I. Echavarri Franco was funded by a grant from "Programa de Excelencia Académica de la DGST, México".

REFERENCES

(1) Chen, L.; McBranch, D. W.; Wang, H.-L.; Helgeson, R.; Wudl, F.; Whitten, D. G. Highly Sensitive Biological and Chemical Sensors Based on Reversible Fluorescence Quenching in a Conjugated Polymer. *Proc. Natl. Acad. Sci. U.S.A.* **1999**, *96*, 12287.

(2) Li, K.; Liu, B. Water-Soluble Conjugated Polymers as the Platform for Protein Sensors. *Polym. Chem.* **2010**, *1*, 252.

(3) Simon, R. A.; Nilsson, K. P. R Optical Reporting by Conjugated Polymers via Conformational Changes. *Springer Ser. Fluoresc.* **2010**, *9*, 389.

(4) Feng, F.; Liu, L.; Yang, Q.; Wang, S. Water-Soluble Conjugated Polymers for Fluorescent-Enzyme Assays. *Macromol. Rapid Commun.* **2010**, *31*, 1405.

(5) Tapia, M. J.; Montserín, M.; Valente, A. J. M.; Burrows, H. D.; Mallavia, R. Binding of Polynucleotides to Conjugated Polyelectrolytes and its Applications in Sensing. *Adv. Colloid Interf. Sci.* **2010**, *158*, 94.

(6) Doré, K.; Dubus, S.; Ho, H.-A.; Lévesque, I.; Brunette, M.; Corbeil, G.; Boissinot, M.; Boivin, G.; Bergeron, M. G.; Boudreau, D.; Leclerc, M. Fluorescent Polymeric Transducer for the Rapid, Simple and Specific Detection of Nucleic Acids at the Zeptomole Level. *J. Am. Chem. Soc.* **2004**, *126*, 4240.

(7) Sigurdson, C. J.; Nilsson, K. P. R; Hornemann, S.; Manco, G.; Polymenidou, M.; Schwarz, P.; Leclerc, M.; Hammarström, P.; Wüthrich, K.; Aguzzi, A. Prion Strain Discrimination Using Luminescent Conjugated Polymers. *Nat. Methods* **2007**, *4*, 1023.

(8) Nilsson, K. P. R; Åslund, A.; Berg, I.; Nyström, S.; Konradsson, P.; Herland, A.; Inganäs, O.; Stabo-Eeg, F.; Lindgren, M.; Westermark, G. T.; Lannfelt, L.; Nilsson, L. N. G.; Hammarström, P. Imaging Distinct Conformational States of Amyloid-β Fibrils in Alzheimer's Disease Using Novel Luminescent Probes. *ACS Chem. Biol.* **2007**, *2*, 553.

(9) Maynor, M. S.; Nelson, T. L.; O'Sullivan, C.; Lavigne, J. J. A Food Freshness Sensor Using the Multistate Response from Analyte-Induced Aggregation of a Cross-Reactive Poly(thiophene). *Org. Lett.* **2007**, *9*, 3217.

(10) Patel, G. N.; Chance, R. R.; Witt, J. D. Visual Conformational Transition in a Polymer Solution. *J. Polym. Sci. C Polym. Lett.* **1978**, *16*, 607.

(11) Lim, K. C.; Heeger, A. J. Spectroscopic and Light Scattering Studies of the Conformational (Rod-to-Coil) Transition of Poly-(Diacetylene) in Solution. *J. Chem. Phys.* **1985**, *82*, 522.

(12) Rawiso, M.; Aimé, J.-P.; Schott, M.; Fave, J.-L.; Schmidt, M.; Muller, G.; Wegner, G. Solutions of Polydiacetylenes in Good and Poor Solvents: A Light and Neutron Scattering Study. *J. Phys. Paris* **1988**, *49*, 861.

(13) Aimé, J.-P.; Bargain, F.; Schott, M.; Eckhardt, H.; Miller, G. G.; Elsenbaumer, R. L. Structural Study of Doped and Undoped Polythiophene in Solution by Small Angle Neutron Scattering. *Phys. Rev. Lett.* **1989**, *62*, 55.

(14) Fave, J.-L.; Schott, M. Sens et implications de la notion de longueur de conjugaison. *J. Chim. Phys.* **1992**, *89*, 931.

(15) Hayakawa, K.; Kwak, J. C. T. Surfactant-Polyelectrolyte Interactions. 1. Binding of Dodecyltrimethylammonium Ions by Sodium Dextran Sulfate and Sodium Poly(styrenesulfonate) in Aqueous Solution in the Presence of Sodium Chloride. *J. Phys. Chem.* **1982**, *86*, 3866.

(16) Malovikova, A.; Hayakawa, K.; Kwak, J. C. T. Surfactant-Polyelectrolyte Interactions. 4. Surfactant Chain Length Dependence of the Binding of Alkylpyridinium Cations to Dextran Sulfate. *J. Phys. Chem.* **1984**, *88*, 1930.

(17) Thalberg, K.; Lindman, B. Interaction between Hyaluronan and Cationic Surfactants. *J. Phys. Chem.* **1989**, *93*, 1478.

(18) Thalberg, K.; Lindman, B.; Bergfeldt, K. Phase Behavior of Systems of Polyacrylate and Cationic Surfactants. *Langmuir* **1991**, *7*, 2893.

(19) Almgren, M.; Hansson, P.; Mukhtar, E.; van Stam, J. Aggregation of Alkyltrimethylammonium Surfactants in Aqueous Poly(styrenesulfonate) Solutions. *Langmuir* **1992**, *8*, 2405.

(20) Kiefer, J. J.; Somasundaran, P.; Ananthapadmanabhan, K. P. Interaction of Tetradecyltrimethylammonium Bromide with Poly-(acrylic acid) and Poly(methacrylic acid). Effect of Charge Density. *Langmuir* **1993**, *9*, 1187.

(21) Hansson, P.; Almgren, M. Interaction of Alkyltrimethylammonium Surfactants with Polyacrylate and Poly(styrene sulfonate) in Aqueous Solution: Phase Behavior and Surfactant Aggregation Numbers. *Langmuir* **1994**, *10*, 2115.

(22) Hansson, P.; Almgren, M. Polyelectrolyte-Induced Micelle Formation of Ionic Surfactants and Binary Surfactant Mixtures Studied by Time-Resolved Fluorescence Quenching. *J. Phys. Chem.* **1995**, *99*, 16684.

(23) Hansson, P.; Almgren, M. Large C_{12}TAB Micelles Formed in Complexes with Polyvinylsulfate and Dextran Sulfate. *J. Phys. Chem.* **1995**, *99*, 16694.

(24) Hansson, P.; Almgren, M. Interaction of CnTAB with Sodium (Carboxymethyl)cellulose: Effect of Polyion Linear Charge Density on Binding Isotherms and Surfactant Aggregation Number. *J. Phys. Chem.* **1996**, *100*, 9038.

(25) *Polymer-Surfactant Systems*; Kwak, J. C. T., Ed.; Marcel Dekker: New York, 1998; Vol. 77.

(26) Konop, A. J.; Colby, R. H. Role of Condensed Counterions in the Thermodynamics of Surfactant Micelle Formation with and without Oppositely Charged Polyelectrolytes. *Langmuir* **1999**, *15*, 58.

(27) Diamant, H.; Andelman, D. Onset of Self-Assembly in Polymer-Surfactant Systems. *Europhys. Lett.* **1999**, *48*, 170.

(28) Diamant, H.; Andelman, D. Self-Assembly in Mixtures of Polymers and Small Associating Molecules. *Macromolecules* **2000**, *33*, 8050.

(29) Hansson, P. Self-Assembly of Ionic Surfactants in Polyelectrolyte Solutions: A Model for Mixtures of Opposite Charge. *Langmuir* **2001**, *17*, 4167.

(30) Wang, C.; Tam, K. C. New Insights on the Interaction Mechanism within Oppositely Charged Polymer/Surfactant Systems. *Langmuir* **2002**, *18*, 6484.

(31) Wang, C.; Tam, K. C. Interaction between Polyelectrolyte and Oppositely Charged Surfactant: Effect of Charge Density. *J. Phys. Chem.* **2004**, *108*, 8976.

(32) Jain, N.; Trabelsi, S.; Guillot, S.; McLoughlin, D.; Langevin, D.; Letellier, P.; Turmine, M. Critical Aggregation Concentration in Mixed Solutions of Anionic Polyelectrolytes and Cationic Surfactants. *Langmuir* **2004**, *20*, 8496.

(33) Wang, C.; Tam, K. C. Interactions between Poly(acrylic acid) and Sodium Dodecyl Sulfate: Isothermal Titration Calorimetric and Surfactant Ion-Selective Electrode Studies. *J. Phys. Chem. B* **2005**, *109*, 5156.
(34) Kuhn, P. S.; Diehl, A. Flexible Polyelectrolyte Conformation in the Presence of Oppositely Charged Surfactants. *Phys. Rev. E* **2007**, *76*, 041807.
(35) Langevin, D. Complexation of Oppositely Charged Polyelectrolytes and Surfactants in Aqueous Solutions. A review. *Adv. Colloid Interf. Sci.* **2009**, *147−148*, 170.
(36) Piculell, L.; Norrman, J.; Svensson, A. V.; Lynch, I.; Bernardes, J. S.; Loh, W. Ionic Surfactants with Polymeric Counterions. *Adv. Colloid Interf. Sci.* **2009**, *147−148*, 228.
(37) Bain, C. D.; Claesson, P. M.; Langevin, D.; Meszaros, R.; Nylander, T.; Stubenrauch, C.; Titmuss, S.; von Klitzing, R. Complexes of Surfactants with Oppositely Charged Polymers at Surfaces and in Bulk. *Adv. Colloid Interf. Sci.* **2010**, *155*, 32.
(38) Kogej, K. Association and Structure Formation in Oppositely Charged Polyelectrolyte−Surfactant Mixtures. *Adv. Colloid Interf. Sci.* **2010**, *158*, 68.
(39) Chen, L.; McBranch, D.; Wang, R.; Whitten, D. Surfactant-Induced Modification of Quenching of Conjugated Polymer Fluorescence by Electron Acceptors: Applications for Chemical Sensing. *Chem. Phys. Lett.* **2000**, *330*, 27.
(40) Chen, L.; Xu, S.; McBranch, D.; Whitten, D. Tuning the Properties of Conjugated Polyelectrolytes through Surfactant Complexation. *J. Am. Chem. Soc.* **2000**, *122*, 9302.
(41) Lavigne, J. J.; Broughton, D. L.; Wilson, J. N.; Erdogan, B.; Bunz, U. H. F. Surfactochromic" Conjugated Polymers: Surfactant Effects on Sugar-Substituted PPEs. *Macromolecules* **2003**, *36*, 7409.
(42) Dalvi-Malhotra, J.; Chen, L. Enhanced Conjugated Polymer Fluorescence Quenching by Dipyridinium-Based Quenchers in the Presence of Surfactant. *J. Phys. Chem. B* **2005**, *109*, 3875.
(43) Gu, Z.; Bao, Y.-J.; Zhang, Y.; Wang, M.; Shen, Q.-D. Anionic Water-Soluble Poly(phenylenevinylene) Alternating Copolymer: High-Efficiency Photoluminescence and Dual Electroluminescence. *Macromolecules* **2006**, *39*, 3125.
(44) Treger, J. S.; Ma, V. Y.; Gao, Y.; Wang, C.-C.; Wang, H.-L.; Johal, M. S. Tuning the Optical Properties of a Water Soluble Cationic PPV: Surfactant Complexation with a Conjugated Polyelectrolyte. *J. Phys. Chem. B* **2008**, *112*, 760.
(45) Thünemann, A. F.; Ruppelt, D. Electroluminescent Polyelectrolyte-Surfactant Complexes. *Langmuir* **2001**, *17*, 5098.
(46) Wosnick, J. H.; Mello, C. M.; Swager, T. M. Synthesis and Application of Poly(phenylene Ethynylene)s for Bioconjugation: A Conjugated Polymer-Based Fluorogenic Probe for Proteases. *J. Am. Chem. Soc.* **2005**, *127*, 3400.
(47) Wu, M.; Kaur, P.; Yue, H.; Clemmens, A. M.; Waldeck, D. H.; Xue, C.; Liu, H. Charge Density Effects on the Aggregation Properties of Poly(p-phenylene-ethynylene)-Based Anionic Polyelectrolytes. *J. Phys. Chem. B* **2008**, *112*, 3300.
(48) Yue, H.; Wu, M.; Xue, C.; Velayudham, S.; Liu, H.; Waldeck, D. H. Evolution in the Supramolecular Complexes between Poly(phenylene-ethynylene)-Based Polyelectrolytes and Octadecyltrimethylammonium Bromide as Revealed by Fluorescence Correlation Spectroscopy. *J. Phys. Chem. B* **2008**, *112*, 8218.
(49) Dou, W.; Wang, C.; Wang, G.; Ma, Q.; Su, X. Enhance Effect of Surfactants on the Photoluminescence and Photostability of Water-Soluble Poly(phenylene ethynylene). *J. Phys. Chem. B* **2008**, *112*, 12681.
(50) Zhang, T.; Fan, H.; Zhou, J.; Jin, Q. Conjugated Polyelectrolyte with Pendant Carboxylate Groups: Synthesis, Photophysics, and pH Responses in the Presence of Surfactants. *J. Polym. Sci., Part A* **2009**, *47*, 3056.
(51) Tapia, M. J.; Burrows, H. D.; Valente, A. J. M.; Pradhan, S.; Scherf, U.; Lobo, V. M. M.; Pina, J.; Seixas de Melo, J. Interaction between the Water Soluble Poly{1,4-phenylene-[9,9-bis(4-phenoxy butylsulfonate)]fluorene-2,7-diyl} Copolymer and Ionic Surfactants Followed by Spectroscopic and Conductivity Measurements. *J. Phys. Chem. B* **2005**, *109*, 19108.
(52) Burrows, H. D.; Lobo, V. M. M.; Pina, J.; Ramos, M. L.; Seixas de Melo, J.; Valente, A. J. M.; Tapia, M. J.; Pradhan, S.; Scherf, U.; Hintschich, S. I.; Rothe, C.; Monkman, A. P. Interactions between Surfactants and {1,4-phenylene-[9,9-bis(4-phenoxy-butylsulfonate)]-fluorene-2,7-diyl}. *Colloids Surf. A* **2005**, *270−271*, 61.
(53) Tapia, M. J.; Burrows, H. D.; Knaapila, M.; Monkman, A. P.; Arroyo, A.; Pradhan, S.; Scherf, U.; Pinazo, A.; Perez, L.; Moran, C. Interaction between the Conjugated Polyelectrolyte Poly{1,4-phenylene[9,9-bis(4-phenoxybutylsulfonate)]fluorene-2,7-diyl} Copolymer and the Lecithin Mimic 1-O-(L-Arginyl)-2,3-O-dilauroyl-sn-glycerol in Aqueous Solution. *Langmuir* **2006**, *22*, 10170.
(54) Burrows, H. D.; Tapia, M. J.; Silva, C. L.; Pais, A. A. C. C.; Fonseca, S. M.; Pina, J.; Seixas de Melo, J.; Wang, Y.; Marques, E. F.; Knaapila, M.; Monkman, A. P.; Garamus, V. M.; Pradhan, S.; Scherf, U. Interplay of Electrostatic and Hydrophobic Effects with Binding of Cationic Gemini Surfactants and a Conjugated Polyanion: Experimental and Molecular Modeling Studies. *J. Phys. Chem. B* **2007**, *111*, 4401.
(55) Monteserin, M.; Burrows, H. D.; Valente, A. J. M.; Lobo, V. M. M.; Mallavia, R.; Tapia, M. J.; Garcia-Zubiri, I. X.; Di Paolo, R. E.; Maçanita, A. L. Modulating the Emission Intensity of Poly-(9,9-bis(6′-N,N,N-trimethylammonium)hexyl)-Fluorene Phenylene) Bromide Through Interaction with Sodium Alkylsulfonate Surfactants. *J. Phys. Chem. B* **2007**, *111*, 13560.
(56) Youk, J. H.; Locklin, J.; Prussia, A.; Advincula, R. Energy Transfer in Poly(3-thiopheneacetic acid) and Oligothiophene Polyelectrolyte-Surfactant Complexes. *Langmuir* **2003**, *19*, 8119.
(57) Lopez-Cabarcos, E.; Rubio-Retama, J.; Sholin, V.; Carter, S. A. Controlling the Photoluminescence of Water-Soluble Conjugated Poly[2-(3-thienyl)ethyloxy-4-butylsulfonate)] for Biosensor Applications. *Polym. Int.* **2007**, *56*, 588.
(58) Laurenti, M.; Rubio-Retama, J.; Garcia-Blanco, F.; Lopez-Cabarcos, E. Influence of the Surfactant Chain Length on the Fluorescence Properties of a Water-Soluble Conjugated Polymer. *Langmuir* **2008**, *24*, 13321.
(59) Yoon, Y.-S.; Park, K.-H.; Lee, J.-C. Self-Assembly Behavior and Optical Properties of Poly(3-thiopheneacetate)/Dialkyldimethylammonium Complexes. *Macromol. Chem. Phys.* **2009**, *210*, 1510.
(60) Yoon, Y.-S.; Kang, H.; Kim, B. G.; Lee, J.-C. Liquid Crystal Alignment Properties of Poly-(3-thiopheneacetate)/ Dialkyldimethylammonium Complexes. *Macromol. Chem. Phys.* **2010**, *211*, 353.
(61) Knaapila, M.; Evans, R. C.; Garamus, V. M.; Almasy, L.; Székely, N. K.; Gutacker, A.; Scherf, U.; Burrows, H. D. Structure and "Surfactochromic" Properties of Conjugated Polyelectrolyte (CPE): Surfactant Complexes between a Cationic Polythiophene and SDS in Water. *Langmuir* **2010**, *26*, 15634.
(62) Wang, D; Moses, D; Bazan, G. C.; Heeger, A. J.; Lal, J. Conformation of a Conjugated Polyelectrolyte in Aqueous Solution: Small Angle Neutron Scattering. *J. Macromol. Sci. A* **2001**, *38*, 1175.
(63) Vallat, P.; Catala, J.-M.; Rawiso, M.; Schosseler, F. Flexible Conjugated Polyelectrolyte Solutions: A Small Angle Scattering Study. *Macromolecules* **2007**, *40*, 3779.
(64) Vallat, P.; Catala, J.-M.; Rawiso, M.; Schosseler, F. Conformational Transitions of Conjugated Annealed Polyelectrolytes. *Europhys. Lett.* **2008**, *82*, 28009.
(65) Nguyen, T.-Q.; Doan, V.; Schwartz, B. J. Conjugated Polymer Aggregates in Solution: Control of Interchain Interactions. *J. Chem. Phys.* **1999**, *110*, 4068.
(66) Schwartz, B. J. Conjugated Polymers as Molecular Materials: How Chain Conformation and Film Morphology Influence Energy Transfer and Interchain Interactions. *Annu. Rev. Phys. Chem.* **2003**, *54*, 141.
(67) Traiphol, R.; Sanguansat, P.; Srikhirin, T.; Kerdcharoen, T.; Osotchan, T. Spectroscopic Study of Photophysical Change in Collapsed Coils of Conjugated Polymers: Effects of Solvent and Temperature. *Macromolecules* **2006**, *39*, 1165.

(68) Traiphol, R.; Charoenthai, N.; Srikhirin, T.; Kerdcharoen, T.; Osotchan, T.; Maturos, T. Chain Organization and Photophysics of Conjugated Polymer in Poor Solvents: Aggregates, Agglomerates and Collapsed Coils. *Polymer* **2007**, *48*, 813.
(69) Traiphol, R.; Charoenthai, N. Effects of Conformational Change and Segmental Aggregation on Photoemission of Illuminophores in Conjugated Polymer MEH-PPV: Blue Shift Versus Red Shift. *Synth. Met.* **2008**, *158*, 135.
(70) Chen, S.-A.; Jen, T.-H.; Lu, H.-H. A Review on the Emitting Species in Conjugated Polymers for Photo- and Electro-luminescence. *J. Chin. Chem. Soc.* **2010**, *57*, 439.
(71) Leese, R. A.; Wehry, E. L. Corrections for Inner-Filter Effects in Fluorescence Quenching Measurements via Right-Angle and Front-Surface Illumination. *Anal. Chem.* **1978**, *50*, 1193.
(72) Gauthier, T. D.; Sham, E. C.; Guerln, W. F.; Rudolf Seltz, W.; Gran, C. L. Fluorescence Quenching Method for Determining Equilibrium Constants for Polycyclic Aromatic Hydrocarbons Binding to Dissolved Humic Materials. *Environ. Sci. Technol.* **1986**, *20*, 1182.
(73) Larsson, T.; Wedborg, M.; Turner, D. Correction of Inner-Filter Effect in Fluorescence Excitation-Emission Matrix Spectrometry Using Raman Scatter. *Anal. Chim. Acta* **2007**, *583*, 357.
(74) Provencher, S. W. A Constrained Regularization Method for Inverting Data Represented by Linear Algebraic or Integral Equations. *Comput. Phys. Commun.* **1982**, *27*, 213. et al. 1982, *27*, 229.
(75) Echavarri Franco, I.; Combet J.; Schosseler F. CNTb, a Set of Scripts for Batch Processing and Statistical Analysis of Photon Correlation Spectroscopy Data via CONTIN Inversion. Hyper Articles en Ligne (HAL), http://hal.archives-ouvertes.fr/hal-00665367.
(76) Cavalier, A.; Spehner, D.; Humbel, B. M. *Handbook of Cryo-Preparation Methods for Electron Microscopy*; CRC Press: Boca Raton, FL, 2008.
(77) Klucker, R.; Munch, J.-P.; Schosseler, F. Combined Static and Dynamic Light Scattering Study of Associating Random Block Copolymers in Solution. *Macromolecules* **1997**, *30*, 3839.
(78) Vallat, P. Synthèse et étude des structures électronique et macromoléculaire d'un polyélectrolyte conjugué: le poly(thiophène 3-acide acétique). PhD dissertation, Université Louis Pasteur: Strasbourg, 2006.
(79) Lapitsky, Y.; Parikh, M.; Kaler, E. W. Calorimetric Determination of Surfactant/Polyelectrolyte Binding Isotherms. *J. Chem. Phys. B* **2007**, *111*, 8379.
(80) Antonietti, M.; Conrad, J.; Thünemann, A. Polyelectrolyte-Surfactant Complexes: A New Type of Solid, Mesomorphous Material. *Macromolecules* **1994**, *27*, 6007.
(81) Claesson, P. M.; Bergström, M.; Dédinaité, A.; Kjellin, M.; Legrand, J.-F.; Grillo, I. Mixtures of Cationic Polyelectrolyte and Anionic Surfactant Studied with Small-Angle Neutron Scattering. *J. Phys. Chem. B* **2000**, *104*, 11689.
(82) Zhou, S.; Hu, H.; Burger, C.; Chu, B. Phase Structural Transitions of Polyelectrolyte-Surfactant Complexes between Poly-(vinylamine hydrochloride) and Oppositely Charged Sodium Alkyl Sulfate. *Macromolecules* **2001**, *34*, 1772.
(83) Bergström, M.; Kjellin, U. R. M.; Claesson, P. M.; Grillo, I. Small Angle Neutron Scattering Study of Mixtures of Cationic Polyelectrolyte and Anionic Surfactant: Effect of Polyelectrolyte Charge Density. *J. Phys. Chem. B* **2004**, *108*, 1874.
(84) Trabelsi, S.; Guillot, S.; Ritacco, H.; Boué, F.; Langevin, D. Nanostructures of Colloidal Complexes Formed in Oppositely Charged Polyelectrolyte/Surfactant Dilute Aqueous Solutions. *Eur. Phys. J. E* **2007**, *23*, 305.
(85) Combet, J. et al., unpublished data.
(86) Emerson, M. F.; Holtzer, A. On the Ionic Strength Dependence of Micelle Number. *J. Phys. Chem.* **1965**, *69*, 3718.
(87) Emerson, M. F.; Holtzer, A. On the Ionic Strength Dependence of Micelle Number. II. *J. Phys. Chem.* **1967**, *71*, 1898.
(88) Zana, R. Ionization of Cationic Micelles: Effect of the Detergent Structure. *J. Colloid Interface Sci.* **1980**, *78*, 330.
(89) Anthony, O.; Zana, R. Interactions between Water-Soluble Polymers and Surfactants: Effect of the Polymer Hydrophobicity. 2. Amphiphilic Polyelectrolytes (Polysoaps). *Langmuir* **1996**, *12*, 3590.
(90) Wang, X.; Li, Y.; Li, J.; Wang, J.; Wang, Y.; Guo, Z.; Yan, H. Salt Effect on the Complex Formation between Polyelectrolyte and Oppositely Charged Surfactant in Aqueous Solution. *J. Phys. Chem. B* **2005**, *109*, 10807.
(91) Wang, H.; Wang, Y. Studies on Interaction of Poly(sodium acrylate) and Poly(sodium styrenesulfonate) with Cationic Surfactants: Effects of Polyelectrolyte Molar Mass, Chain Flexibility, and Surfactant Architecture. *J. Phys. Chem. B* **2010**, *114*, 10409.
(92) Mel'nikov, S. M.; Sergeyev, V. G.; Yoshikawa, K. Discrete Coil-Globule Transition of Large DNA Induced by Cationic Surfactant. *J. Am. Chem. Soc.* **1995**, *117*, 2401.
(93) Mel'nikov, S. M.; Sergeyev, V. G.; Yoshikawa, K. Transition of Double-Stranded DNA Chains between Random Coil and Compact Globule States Induced by Cooperative Binding of Cationic Surfactant. *J. Am. Chem. Soc.* **1995**, *117*, 9951.
(94) Shirahama, K. The Nature of Polymer-Surfactant Interactions. In *Polymer-Surfactant Systems*; Kwak, J. C. T., Ed.; Marcel Dekker: New York, 1998; Vol. *77*.